Design and Locomotion Control of a Myliobatid-inspired Robot Actuated by Passively-flexing Pectoral Fins

Songzi Guo[1], Zhiyin Li[1] and Jinhua Zhang[2]
[1]*China Ship Design and Development Center, Wu'han 430034, China*
[2]*Key Laboratory of Education, Ministry for Modern Design and Rotor-Bearing System, Xi'an Jiaotong University, Xi'an 710049, China*

Keywords: Bionic Design, Robot Fish, Flexible Pectoral Fin, Bio-Inspire.

Abstract: This article proposes the mechanical design of a myliobatid-inspired robot (XJRoman-I) based on oscillatory swimming mechanism for both stability and agile manoeuvrability. Inspired by anatomical studies, a pair of passively bending pectoral fins are developed to generate propulsive force for the prototype. An elevator is adopted to adjust its pitch attitude. Primary experimental research on the effect of fin's spanwise stiffness on swimming performance is performed to improve its swimming performance. By embedding a stiff rod into the fin's leading edge, the thrust and lateral force generated by the fins are improved significantly. Finally, a CPG-based control method is introduced to make the prototype achieve different locomotion patterns including cruising by flapping pectoral fins and turning by modulating phase relation of pectoral fins. This paper mainly focuses on propulsive capability of stability and agility for the prototype, and expects to propose an excellent underwater vehicle covering wide range of applications.

1 INTRODUCTION

Traditional underwater vehicles play an important role in underwater explorations. But with the growing demands for pelagic and deep-sea missions, they couldn't well adapt to these complex and challengeable operating scenarios because of limitation of their propulsive mechanisms. Hence, in order to solve this conundrum, biologists and engineers attempt to mimic propulsive mechanisms of marine animals to enhance the performance of underwater vehicles. Admittedly, marine animals are quite different from underwater vehicles in many aspects. Yet even so, by understanding how aquatic animals achieve these inborn advantages, engineers can be inspired to develop a variety of novel undersea robots like a robotic dolphin (Yu, 2017), knife-fish (Liu, 2017) and trout (Takemura, 2011) giving man's horizon further into the ocean than ever before.

Among the numerous aquatic animals, myliobatid, renowned as a large open-water swimmer, has streamlined body shape and peculiar propulsive mechanism (Rosenberger, 2001). While the majority of fishes use their caudal fin to generate propulsion and pectoral fins to keep balance, rays synchronically or asynchronously flap their flexible pectoral fins on each side of the body to achieve agile manoeuvre and stable locomotion, which take great advantages over other caudal fin-based fishes in long-distance swimming (Breder,1926) and agile motion (Fish,2018).

Researchers intensively investigated kinematics characteristics of myliobatid fishes, attempting to reveal the mechanism behind such great comprehensive abilities of high efficiency and stability during cruise. By analysing the typical frames of a cruising manta ray, Liu et al (Liu, 2015) established a kinematics model to delineate deformation of pectoral fins in both span and chord. The model indicated that the deformation in the span becomes significantly at distal part of pectoral fins. The flexible deformation in span was proved to allow mantas to perform small radius turns with its ratio as high as 67 deg/s (Fish et al., 2018), despite their rigid body (Parson, 2011). Based on the kinematics research on mantas, various computational hydrodynamic simulations (Fish et al., 2016) were carried out and indicated that the flexible distal part of pectoral fins plays an essential role in mantas' swimming and generates the majority of thrust. On top of this, comprehensive experimental studies were carried out by Clark and Smits (Clark et al, 2006).

Guo, S., Li, Z. and Zhang, J.
Design and Locomotion Control of a Myliobatid-inspired Robot Actuated by Passively-flexing Pectoral Fins.
DOI: 10.5220/0010857000003271
In *Proceedings of the 19th International Conference on Informatics in Control, Automation and Robotics (ICINCO 2022)*, pages 353-360
ISBN: 978-989-758-585-2; ISSN: 2184-2809

They found the efficiency of a flapping foil is promoted by flexibility distributed on the foil. With the help of DPIV technology, Dewey et al (Dewey et al., 2012; 2013) observed wake topology formed by a bionic pectoral fin and proposed a resonance theory, which indicated a maximal efficiency is always achieved while flapping pectoral fins is actuated under its resonance frequencies.

By mimicking the kinematics features of oscillatory batoid fishes, many newly-designed underwater robots have been developed. In 2011, a ray-like robot fish was initially design and fabricated by Low et al (Low, 2012), whose pectoral fin in one side was actuated by three servos in parallel. Similarly, this parallel connected actuating system was also utilized by an improved ray-like robot (Cao, 2019). A cpg-fuzzy-based control method was introduced to better mimic the swimming gaits of myliobatid. However, the robot fish can actively control multiple degrees of freedom along the chord by means of groups of servos, redundant actuators lead to extra loss of mechanical energy and limit swimming performance of robots. Therefore, Chew et al (Chew, 2016) have developed a manta-like robot merely actuated by two servos. Because of the lightweight and compact design, maximal swimming speed of this robot fish can reach to 1.7 body length per second.

In this paper, the design of a myliobatid-inspired robot equipped with a pair of passively bending pectoral fins based on oscillatory swimming mechanism is proposed. The fin's design is based on the anatomical structure of an eagle-ray. A traveling wave alone the chord, coupling with a vertical wave alone the wingspan is presented on the flexible fin during flapping in the water. In addition, an experiment on the effect of span-wise stiffness is carried out to improve the swimming performance of the prototype. Finally, the prototype equipped with the optimized pectoral fins is tested in a pool to verify its capability of locomotion.

2 FROM BIOMIMETIC SUBJECT TO BIOINSPIRED ROBOT

2.1 Overview of the Prototype

To mimic stable and flexible swimming mode of myliobatid, a bionic oscillatory robot equipped with a pair of flexible pectoral fins is constructed, as shown in Figure1(a). The robot prototype has a flat and streamlined body shape suitable to achieve both fast and stable motions in the water and equip with a pair of flexible pectoral fins, and can be divided into four parts: (1) a head cabinet fixing two of actuating servos (Omg, 40kgf.cm) providing torque force for the bionic fins; (2) a central waterproof shell containing electric components; (3) an elevator to adjust pitch attitude; (4) a pair of flexible pectoral fins providing propulsive force for the prototype. The head cabinet as well as the central shell are made of the lightweight material (nylon-12), whose density is close to water. The weight of the robot is 680g, and it can provide an extra load capacity of 200g. A central controller (RoboMaster, DJI) powered by FreeRTOS system is adopted to control locomotion of the prototype. Considering that the effect of attenuation for signals will be intensive with the increasing frequency in the water, a radio module with lower transmission frequency is adopted as communication unit. Additionally, the central waterproof shell accommodates sensors for underwater environment perception. An inertial measurement unit (IMU) embedded in the controller is arranged in parallel with the robot principle axis to sense the three-dimensional attitude for the prototype with a sampling rate of 50 Hz. A developed pressure sensor MS5837 is mounted at the end of the shell to gauge hydraulic pressure corresponding to the depth where the robot stays. It has a 0.2mbar resolution in a scale range of 0-30bar. The elevator at the stern of the prototype driven by a servo performs vertical rotation to provide pitch torque for the prototype.

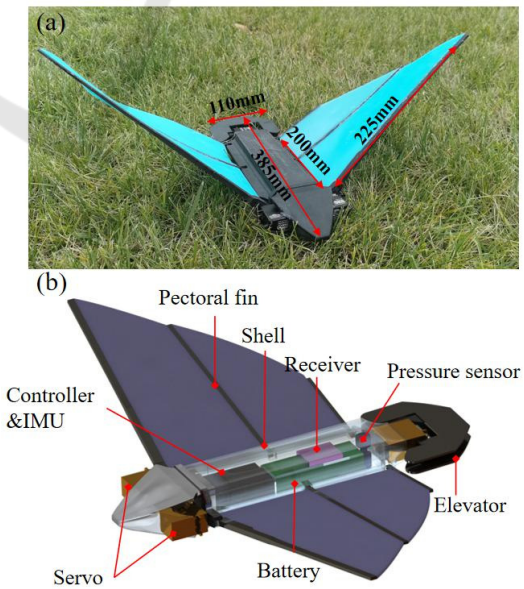

Figure 1: (a) Isometric view of the robotic prototype. (b) Components of the robot prototype.

Table 1: Main Technical Specifications of the Robotic Prototype.

Items	Characteristics
Dimension	385mm×560mm×50mm
Total mass	680g
Control unit	STM32F407IGH
Sensors	IMU(BMI088), Pressure sensor
Drive units	Servo×3(waterproof)
Communication unit	AS32170-170MHz
Power supply	11.1V(2200mAh-Li)

2.2 Design and Fabrication of Bionic Pectoral Fins

The design of the bionic pectoral fin is based on the anatomical details of a myliobatid swimmer, eagle-ray. It is a typical swimmer using oscillatory model embodying an excellent balance between manoeuvrability and efficiency. For this reason, their anatomical characteristics would inspire the design of next-generation underwater vehicles. To uncover the outstanding swimming performance of eagle-rays, we conduced anatomical experiments on its pectoral fins to discover the smallest detail in musculoskeletal structure, which is shown in Figure2.

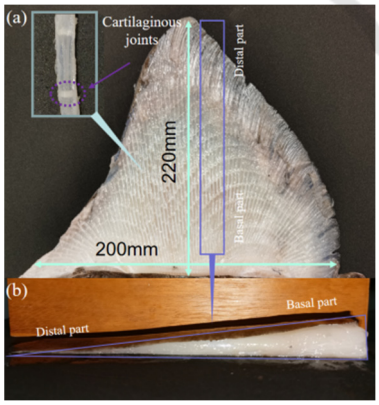

Figure 2: (a) The fin's skeletal structure of an eagle-ray. (b) The cross-section of the dissected pectoral fin.

The pectoral fin of the eagle-ray is approximately 200 mm in chord and 220 mm in span, where span is measured from the fin tip to the root. The fin's aspect-ratio is close to 2.2 that is the ratio of the span-wise length to the fin's surficial area.

After removing tissues from the specimen, skeletal structure can be clearly observed in Figure2(a). The pectoral fin consists of an array of 175 fin-rays. Each of the fin-ray is composed by several segments connected by cartilaginous joints. These segments extend out from the root to the edge of the pectoral fin and arrange in radial formation. In Figure2(b), the thickness of the pectoral fin decreases from the basal part to the distal part. This kind of skeletal and muscular structure is considered to be favourable for the range of motion for fins tip, by which agility and efficiency of eagle-rays can be enhanced. Additionally, skeletal connections also exist between the adjacent radial segments. This connective tissue is termed cross-bracing, which can limit the oscillatory amplitude of adjacent fin-rays and increase the chord-wise stiffness in the pectoral fin necessary for the transmission of traveling wave along the chord-wise direction.

Based on the morphologic characteristics and anatomical details of the specimen, the design of a bionic pectoral fin to mimic the oscillatory propulsion mechanism is proposed. The chord-length and span-length of the bionic fin are 220mm and 200mm, respectively. The AR of the bionic fin is about 2.2.

The leading edge that has the longest length among fin-rays connects with a servo (Omg, 40kgf.cm), providing oscillatory force for the pectoral fin. The rest of the fin-rays at the middle and the end of the bionic pectoral fin respectively can passively control the wavelength alone the chord presenting on the pectoral fin. To make the bionic pectoral fin achieve passive deformation alone the wingspan and allow the flexible membranes to maintain it shape while flapping in the water, all of the fin-rays are made of nylon with high-ductility. The thickness of the fin-rays decreases from the basal part to the distal part. Therefore, the tip of the pectoral fin can achieve more significant deformation than proximal part. Two of the flexible membranes are made of silicon rubber and attached to the fin-rays by adhesive (E41, Wacker). Since M4601, a kind of two-component silicone rubber, has appropriate tensile strength (6.5N/mm^2) and lower hardness (28A) compared with other silicon rubbers, it is adopted to fabricate flexible membranes for the bionic pectoral fins. Firstly, the unmixed M4601-A and M4601-B are poured into a container by weight of 1:9. After degassing in a vacuum chamber, the mixed material is poured into resin moulds where the demould releaser has been sprayed. And then, after curing at room temperature for 12 hours, the vulcanized specimen is stripped from the moulds. The cured fin-like membranes have 2mm in thickness. Finally,

when all of the compliant membranes are fabricated. They are adhered to the compliant fin-rays. The fabricated bionic pectoral fin is shown in Figure3.

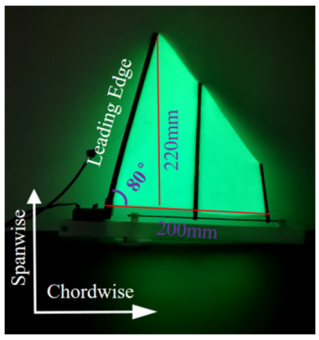

Figure 3: The fabricated bionic pectoral fin, noted that in this paper the bionic fins are dyed into different colours by fluorescent agent to make them more distinguishable.

2.3 Experiment on Bionic Pectoral Fins

In order to improve propulsive performance for the robot, experimental research was carried out to investigate the effect of stiffness distribution along the leading edge on thrust and lateral force generated by the pectoral fins. On top of that, the position of the passive bending along the leading edge is investigated, since it determines the proportion of the distal part on the bionic fin, which has been proved to be closely relative to thrust generation in Fish's work (Fish, 2016).

In the experiment, we studied five bionic fin's configurations whose leading edge is different in the proportion of high stiffness part marked with a red bracket in Figure4(a). An aluminium rod is embedded into the rear side of fin's leading edge to form discrete region with high stiffness along the span-wise direction. The fabricated bionic fins are demonstrated in Figure4(b) where the proportion of the high stiffness part decreases from 1 (the pink pectoral fin) to 0 (dull-red pectoral fin). In the fins' naming scheme, 'HS-*' refers to the proportion of the leading edge with high stiffness part.S

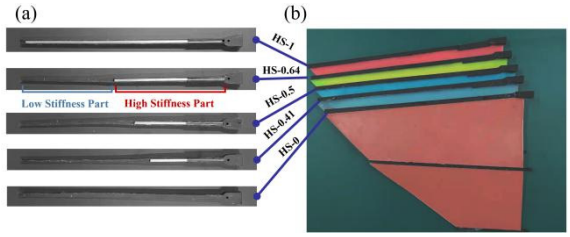

Figure 4: (a) The leading edges embedded with different length of aluminium rods. (b) The five fabricated bionic fins with different scale of high stiffness region.

The experimental apparatus is shown in Figure5. A servo clamped by a carriage was used to actuate the bionic fins. The flapping apparatus is mounted on the interface of a 6-axis force torque sensor (ATI-Mini40, 0~20N) and submerged in a water tank. Since the passive bending appearing on the leading edge is critical to the thrust generation, a high-speed camera (Phantom, v1612) was placed in the front of the water tank to capture the frames to investigate the passive bending appearing on the leading edge during flapping.

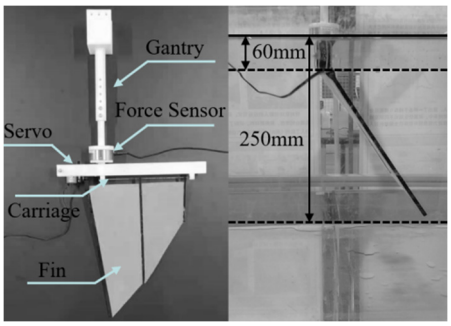

Figure 5: Annotated diagram of the experimental apparatus.

Myliobatid prefers to change the flapping frequency to meet different motion requirements (Fish, 2016). Therefore, the five bionic fins were actuated under different stroke frequencies from 0.3 to 1.0 Hz with a constant flapping amplitude of 80°. To make the experimental data acquired in our work reliable, the collecting duration of each set of data were lasting for 20 flapping circles. The thrust and lateral force throughout ten stable flapping circles were selected to obtain the averaged thrust and lateral force.

Cycle-averaged thrust and lateral force generated by the bionic fins are shown in Figure6(a) and Figure6(b), respectively. Compared with the bionic fin's configuration HS-0 (Dull-red) without stiffener in the leading edge, the other fin's configurations have overall increases in averaged thrust and lateral force. Additionally, except for the bionic fin termed HS-1 (Pink), the averaged thrust increases with the increasing stoke frequency before a turning point, where the averaged thrust reaches its maximum and then starts to decrease. On the other hand, the averaged lateral force demonstrates incremental trend with the increasing stroke frequency. The fin's configuration HS-1 embedded with a stiff rod as long as its leading edge can achieve the highest cycle-averaged thrust among the fin's design, which is 1.32N at stroke frequency of 1.0 Hz. However, its generated lateral force can't be ignored. Because a pair of bionic pectoral fins mounted on the robot

prototype couldn't be perfectly symmetrical in size, the discrepancy in lateral force make the prototype difficult to keep its course. If the fundamental need for the robot prototype is to perform cursing locomotion that focuses on the swimming speed and stability, the ideal pectoral fins are expected to provide a significant thrust but relatively unobvious magnitude of lateral force to maintain the swimming stability. Based on the experimental result, the HS-0.5 (blue) is chosen as an ideal actuator for the robot prototype, as it can achieve great averaged forces even closer to that of the HS-1 at stroke frequencies from 0.3 Hz to 0.7Hz while the averaged lateral forces are relatively lower than other pectoral fins.

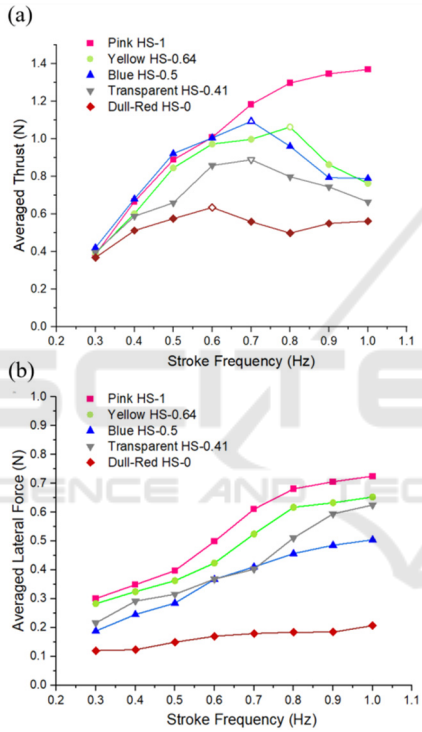

Figure 6: (a) The cycle-averaged thrust and (b) the lateral force at different stroke frequencies from 0.3 Hz to 1.0 Hz. The hollow symbol demonstrates the stroke frequency climbs to the turning point, where the averaged thrust begins to drop down for the next stroke frequency.

While a bionic fin is flapping, the position of a passively-bending point along the fin's leading edge marked with a couple of red arrows in Figure7 can serve as an indicator for the magnitude of hydrodynamic load on the bionic fin, which is relative to the force generation of the bionic fin. Therefore, the image data acquired from the high-speed camera were analysed to obtain the position of the passively-bending points.

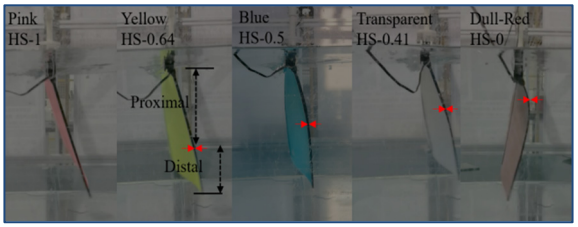

Figure 7: The snapshots of the different designs of bionic fins while actuating at stroke frequency of 1 Hz. The passively-bending points are mark with red arrows.

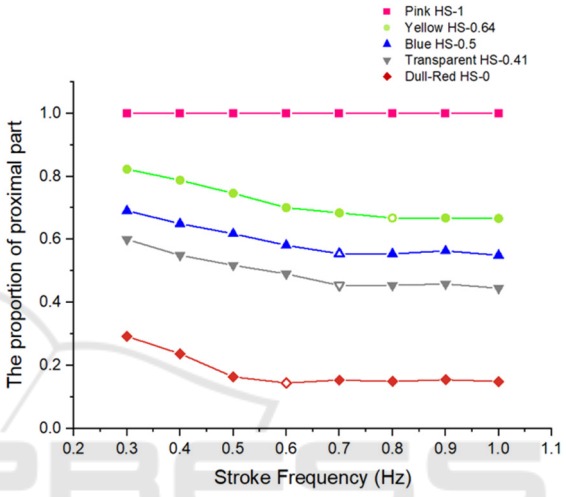

Figure 8: The proximal stiff part occurring on the bionic fin. The hollow symbol demonstrates the stroke frequency where the variation tendency in the chart is changed.

The proportion of the proximal stiff part occurring on the bionic fin is shown in Figure8. For the fin's configuration of HS-1.0 (Pink), the passive bending didn't appear on its leading edge, as the leading edge of the fin is rigid enough to resist the reactive force. In contrast, the proximal stiff part of the other bionic fins decreases with the stroke frequency increasing because of the increasing hydrodynamic load on the fin. However, as the stroke frequency further increases to a restraint frequency, the proportion of the proximal part begins to keep a constant value. It is because the embedded aluminium rod commences to restrain the passively-bending point from shifting towards proximal part further,

It should be noted that compared with Figure6(a) and Figure8, the bionic fins reach their maximum in averaged thrust as the proportion of the proximal part just drop down to its bottom. For the next stroke frequency, the generated thrust begins to decrease. We deduce that the distal part on the bionic fin ploys an important role in thrust generation. While the stroke frequency increases from 0.3 Hz to the trans-

frequency, the increment in thrust takes advantage over the increment in drag force. Hence, the gross magnitude of the thrust shows a growing trend. On the contrary, while stroke frequency increases beyond the trans-frequency, the increment in drag force takes advantage over the increment in thrust, since the scale that can generate thrust is restrained.

3 LOCOMOTION CONTROL BASED ON A CPG-BASED CONTROL METHOD

Owing to central pattern generators (CPGs) modulating the rhythmic movements, animals can perform various locomotion patterns with excellent stability. They can be also employed to control coordination locomotion of robots with multi-degree of freedom especially in performing swimming patterns of robotic fish and other types of robots (Zhou and Low, 2012). Many sorts of the CPG models have been employed to control locomotion for bio-inspired robots, such as Hopf model (Zhou and Low, 2010a), Matsuoka's model (Matsuoka, 1985) and Ijspeert's model (Ijspeert et al., 2007). In this paper, we adopt a simplified linear CPG model proposed by (Wang et al., 2017) to generate rhythmic signals for three servomotors corresponding to the fins and the tail. The CPG controller shown in Figure 9 is composed of three coupled oscillators and it is implemented as follows:

$$\begin{cases} \dot{a}_i = \eta_i (A_i - a_i) \\ \dot{b}_i = \beta_i (B_i - b_i) \\ \dot{x}_i = 2\pi f_i + \sum_{j \in I_i} \mu_{ij} (x_j - x_i - \varphi_{ij}) \\ \theta_i = b_i + a_i \cos(x_i) \end{cases} \quad (1)$$

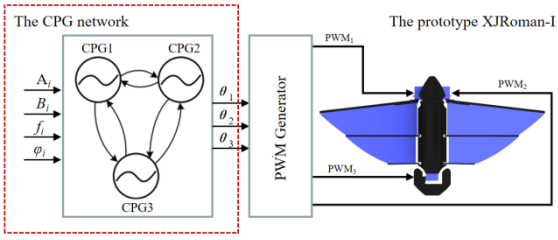

Figure 9: The CPG network of XJRoman-I.

The parameters a_i, b_i and x_i are state variables of the CPG model and represent the amplitude, offset and phase of the rhythmic signal produced by the ith oscillator. A_i, B_i and f_i are control parameters to modulate the desired flapping amplitude, offset and frequency. φ_{ij} is a parameter for the desired phase relation between the ith oscillator and jth oscillator. μ_{ij} is a coefficient denoting the coupling strength between the ith oscillator and jth oscillator. η_i and β_i are converging coefficient affecting the convergence speed of the CPG network. The output θ_i is the input angle of the servomotor. The subscripts i=1, 2, 3 correspond to the left pectoral fin, right pectoral fin and the tail of the prototype, respectively

4 SWIMMING TEST FOR THE PROTOTYPE

In order to acquire cruise speed of the prototype, we tested the prototype equipped with the blue pectoral fins (HS-0.5) in a swimming pool under stroke frequencies from 0.5 Hz to 1.2 Hz with a fixed flapping amplitude (80°). In cruise pattern (Figure10), CPG1 and CPG2 modulate synchronous rhythm signals to actuate pectoral fins to keep the robot swimming along the straight course. While actuated at the a stroke frequency of 0.8 Hz, the prototype can reach its maximal cruising speed at 1.8 BL/s (body length per second).

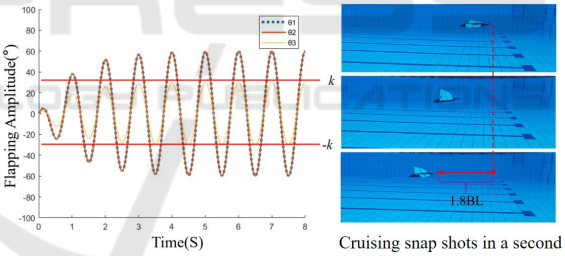

Figure 10: Output signals of the CPGs while the prototype performing cruise locomotion.

Table 2: Parameter Values in CPGs (Cruise Pattern).

f_i	φ_{ij}	A_i	B_i	α_i	β_i	μ_{ij}
[1,1,1]	0	[60,60,k]	[0,0,0]	[1,1,1]	[1,1,1]	1

In turning pattern, The modulated signals are recorded in Figure11, where the CPG1 and CPG2 modulate asynchronous rhythm signals to actuate the pectoral fins asynchronously to alter swimming course of the robot gradually. Based on the snap shots of the turning pattern, the CPG-based controller can make the prototype alter swimming gaits stably.

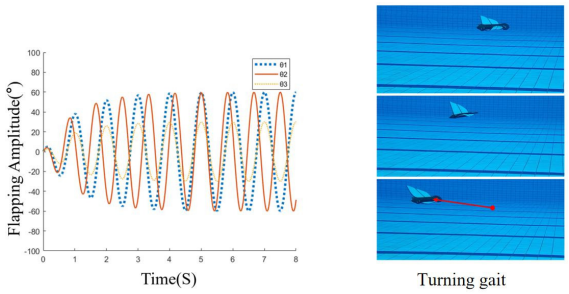

Figure 11: Output signals of the CPGs while the prototype performs turning gait.

Table 3: Parameter Values in CPGs (TurningPattern).

f_i	φ_{ij}	A_i	B_i	α_i	β_i	μ_{ij}
[1,1.2,1]	0	[60,60,k]	[0,0,0]	[1,1,1]	[1,1,1]	1

5 POTENTIAL ONGOING WORK

In further work, we are going to investigate propulsive efficiency of the robot prototype, since it is a critical parameter to evaluate the swimming performance of the prototype, especially in fulfilling long-distance mission.

On the other hand, since the flapping bionic fin can also provide lift force for the robot, it can be used to achieve gliding locomotion for the prototype to save energy during swimming. In our further work, we also plan to investigate the gliding locomotion for the prototype to make it fulfil a long-distance travel.

6 CONCLUSION

In this study, a prototype of oscillatory robot based on the combination of biological swimming mechanisms and morphological features was proposed to make the prototype achieve both fast and stable locomotion through a pair of bionic pectoral fins. Moreover, primary research on the effect of fin's span-wise stiffness on the propulsion performance was carried out. The experiment investigated the thrust and lateral force generation of five fin designs embedded with different length of aluminum rods. The experimental result shows that embedding a stiff rod into the fin's leading edge can cause the thrust and lateral force to improve significantly at stroke frequency beyond 0.5Hz; up to 138% increasement in thrust for the HS-1 (pink) relative to HS-0. In addition, the result also suggests that the bionic fin named HS-0.5 (blue) takes advantage over other designs in capacity of achieving stable and fast motion for the prototype.

The fast motion performed by the prototype shows the passively-flexing pectoral fin proposed in our research is an excellent candidate for underwater propulsive mechanism.

ACKNOWLEDGEMENTS

This research was financially supported by the National Nature Science Foundation of China (No. 91748123).

REFERENCES

Yu, J., Liu, J., Wu, Z., & Fang, H.. (2017). Depth control of a bioinspired robotic dolphin based on sliding mode fuzzy control method. IEEE Transactions on Industrial Electronics, 1-1.

Liu, H., Taylor, B., & Curet, O. M.. (2017). Fin ray stiffness and fin morphology control ribbon-fin-based propulsion. Soft Robot, 103-116.

Rosenberger, L. J.. (2001). Pectoral fin locomotion in batoid fishes: undulation versus oscillation. Journal of Experimental Biology, 204(Pt 2), 379-394.

Takemura, R., Akiyama, Y., Hoshino, T., & Morishima, K.. (2011). Chemical switching of jellyfish-shaped micro robot consisting only of cardiomyocyte gel. Solid-state Sensors, Actuators & Microsystems Conference. IEEE.

Breder, C. M. (1926). The locomotion of fishes. Zoologica,4.

Fish, F. E., Kolpas, A., Crossett, A., Dudas, M. A., & Bart-Smith, H.. (2018). Kinematics of swimming of the manta ray: three-dimensional analysis of open-water maneuverability. Journal of Experimental Biology, 221(Pt 6), jeb.166041.

Low, K. H., Zhou, C., Seet, G., Bi, S., & Cai, Y.. (2012). Improvement and testing of a robotic manta ray (RoMan-III). IEEE International Conference on Robotics & Biomimetics. IEEE.

Cao, Y., Lu, Y., Cai, Y., Bi, S., & Pan, G.. (2019). Cpg-fuzzy-based control of a cownose-ray-like fish robot. Industrial Robot, ahead-of-print(ahead-of-print).

Liu, G., Ren, Y., Zhu, J., Bart-Smith, H., & Dong, H.. (2015). Thrust producing mechanisms in ray-inspired underwater vehicle propulsion. Theoretical and Applied Mechanics Letters, 5(001), 54-57.

Fish, F. E., Kolpas, A., Crossett, A., Dudas, M. A., & Bart-Smith, H.. (2018). Kinematics of swimming of the manta ray: three-dimensional analysis of open-water maneuverability. Journal of Experimental Biology, 221(Pt 6), jeb.166041.

Parson, J. M., Fish, F. E., & Nicastro, A. J.. (2011). Turning performance of batoids: limitations of a rigid body.

Journal of Experimental Marine Biology & Ecology, 402(1-2), 12-18.

Fish, F.E., Schreiber, C.M., Moored, K.W., Liu, G., Dong, H.and Bart Smith, H. (2016), "Hydrodynamic performance of aquatic flapping: efficiency of underwater flight in the manta", Aerospace, Vol. 3 No. 3, pp. 1-24.

Clark, R. P., & Smits, A. J., (2006). Thrust production and wake structure of a batoid-inspired oscillating fin. Journal of Fluid Mechanics, 562(562), 415-429.

Dewey, P. A., Carriou, A., & Smits, A. J., (2012). On the relationship between efficiency and wake structure of a batoid-inspired oscillating fin. Journal of Fluid Mechanics, 691, 245-266.

Dewey, P. A., Boschitsch, B. M., Moored, K. W., Stone, H. A., & Smits, A. J., (2013). Scaling laws for the thrust production of flexible pitching panels. JOURNAL OF FLUID MECHANICS, 732, 29-46.

Chew, C. M., Lim, Q. Y., & Yeo, K. S. (2016). Development of propulsion mechanism for Robot Manta Ray. IEEE International Conference on Robotics & Biomimetics. IEEE.

Wang, W., Gu, D., & Xie, G. (2017). Autonomous optimization of swimming gait in a fish robot with multiple onboard sensors. IEEE Transactions on Systems Man & Cybernetics Systems, 1-13.

Zhou, C.L. and Low, K.H. (2012). Design and locomotion control of a biomimetic underwater vehicle with fin propulsion. IEEE/ASME Transactions on Mechatronics, Vol. 17 No. 1, pp. 25-35.

Zhou, C.L. and Low, K.H. (2010a). Better endurance and load capacity: an improved design of manta ray robot (RoManII). Journal of Bionic Engineering, Vol. 7 No. S4, pp. S137-S144.

Matsuoka, K. (1985). Sustained oscillations generated by mutually inhibiting neurons with adaptation. Biological Cybernetics, Vol. 52 No. 6, pp. 367-376.

Ijspeert, A.J., Crespi, A., Ryczko, D. and Cabelguen, J.-M. (2007). From swimming to walking with a salamander robot driven by a spinal cord model. Science, Vol. 315 No. 5817, pp. 1416-1420.